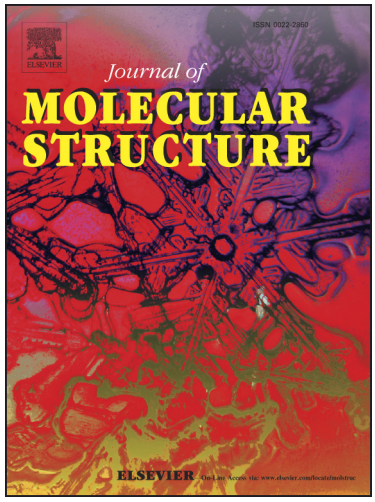

Phase behavior and crystal structure of 3-(1-naphthyloxy)- and 3-(4-indolyloxy)-propane-1,2-diol, synthetic precursors of chiral drugs propranolol and pindolol

Alexander A. Bredikhin, Aidar T. Gubaidullin, Zemfira A. Bredikhina, Robert R. Fayzullin, Aida I. Samigullina, Dmitry V. Zakharychev

PII: S0022-2860(13)00303-7
DOI: http://dx.doi.org/10.1016/j.molstruc.2013.04.018
Reference: MOLSTR 19673

To appear in: *Journal of Molecular Structure*

Received Date: 20 February 2013
Revised Date: 29 March 2013
Accepted Date: 1 April 2013

Please cite this article as: A.A. Bredikhin, A.T. Gubaidullin, Z.A. Bredikhina, R.R. Fayzullin, A.I. Samigullina, D.V. Zakharychev, Phase behavior and crystal structure of 3-(1-naphthyloxy)- and 3-(4-indolyloxy)-propane-1,2-diol, synthetic precursors of chiral drugs propranolol and pindolol, *Journal of Molecular Structure* (2013), doi: http://dx.doi.org/10.1016/j.molstruc.2013.04.018

Phase behavior and crystal structure of 3-(1-naphthyloxy)- and 3-(4-indolyloxy)-propane-1,2-diol, synthetic precursors of chiral drugs propranolol and pindolol

Alexander A. Bredikhin, Aidar T. Gubaidullin, Zemfira A. Bredikhina, Robert R. Fayzullin, Aida I. Samigullina and Dmitry V. Zakharychev

A.E. Arbuzov Institute of Organic and Physical Chemistry, Kazan Scientific Center, Russian Academy of Sciences, Arbuzov St., 8, Kazan 420088, Russian Federation

Abstract: Valuable precursors of popular chiral drugs propranolol and pindolol, 3-(1-naphthyloxy)-propane-1,2-diol **3** and 3-(4-indolyloxy)-propane-1,2-diol **4** were investigated by IR spectroscopy, DSC, and X-ray diffraction methods. Both compounds, crystallizing from enantiopure feed material, form "guaifenesin-like" crystal packing in which the classic H-bonded bilayers, framed in both sides by hydrophobic fragments of the molecules, acts as the basic crystal-forming motif. Diol **4** prone to spontaneous resolution and conserves its packing pattern crystallizing from racemate. Under the same conditions, diol **3** forms weakly stable solid racemic compound. Some reasons for such a behavior are identified and discussed.

Keywords: Propranolol; Pindolol; Thermochemical data; Single crystal X-ray analysis; Chirality driven crystallization; Crystal packing.

1. Introduction

Non-specific β-blockers propranolol **1** [1a] and pindolol **2** [1b] are among the top in its class, pindolol, except adrenergic activity, shows the properties of serotonin $5HT_{1A}$-receptor antagonist.

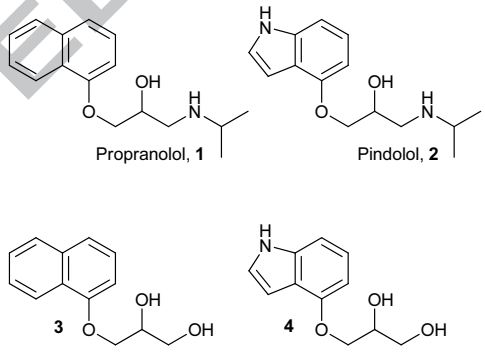

Scheme 1.

Both propranolol and pindolol have pronounced stereoselectivity of biological activity [2-4], and for this reason there is a need to obtain these substances in the single enantiomer form. The study of the phase diagrams of these compounds showed that propranolol forms a racemic compound in the crystalline phase. Moreover, propranolol belongs to the type of "anticonglomerates", i.e. substances for which the dome of the phase diagram "temperature of fusion (T^f) - enantiomeric composition (x)" with a maximum at x = 0.5 occupies almost the entire phase diagram [5,6]. As for the pindolol, according to thermochemical data in the

solid phase, it forms a continuous non-ideal solid solution with a very pronounced maximum at x = 0.5 [5]. In both cases, the features of the phase behavior of **1** and **2** make it very difficult (not to say - make it impossible) to achieve high enantiomeric purity of their solid samples by recrystallization. Consequently, the high enantiomeric purity of the final products should be provided at the stage of nonracemic precursor's preparation. The aim of this work is to study the phase behavior and crystal structure of the glycerol ethers **3** and **4**. Compound **3**, 3-(1-naphthyloxy)-propane-1,2-diol, has previously been used as a synthetic precursor of non-racemic propranolol [7,8]. For compound **4**, 3-(4-indolyloxy)-propane-1,2-diol, the references [9,10] contain description of synthetic reactions that can lead to the non-racemic pindolol. The structures of compounds 1-4 are shown in Scheme 1.

2. Experimental

2.1. Instrumentation

The NMR spectra (399.9 MHz for ^{1}H and 100.5 MHz for ^{13}C) were recorded on a Bruker Avance-400 spectrometer with TMS as the internal standard. The IR spectra of the polycrystalline samples of *rac*- and *scal*-compounds under investigations in KBr pellets were recorded on a Bruker IFS-66v Fourier-transform spectrometer. Optical rotations were measured on a Perkin-Elmer model 341 polarimeter (concentration *c* is given as g/100 ml). Melting points for general purposes were determined using a Boëtius apparatus and are uncorrected. Enantiomeric purity was checked by HPLC analysis performed on a Shimadzu LC-20AD system controller. All thermal measurements were performed on a Perkin-Elmer Diamond DSC model in aluminum pans using a heating rate of 10 K min^{-1}. The mass of the samples amounted to approximately 1.0 mg was measured by a Sartorius CPAQ-2P microbalance, the measurement resolution is 1 μg. Both temperature scale and heat flux were calibrated against the data for indium and naphthalene.

2.2. Materials

Racemic epichlorohydrin, 3-chloropropane-1,2-diol, 1-naphthol and 4-hydroxyindole were commercially available. Nonracemic 3-chloro-1,2-propanediols were prepared through Jacobsen kinetic hydrolytic resolution of *rac*-epichlorohydrin [11]. Racemic and (*S*)-diols **3** were synthesized by analogy with the published procedure [12] from 1-naphthol (10 mmol) and *rac*- or (*S*)-3-chloropropane-1,2-diol (1.3 g, 12 mmol), respectively:

***rac*-3-(1-Naphthyloxy)-propane-1,2-diol, *rac*-3.** Yield: 1.7 g (78 %), mp 98-100 ^{o}C (hexane) {lit. [8]: mp 99-101 ^{o}C}.

(*S*)-3-(1-Naphthyloxy)-propane-1,2-diol, (*S*)-3. Yield: 1.6 g (73 %), mp 111-113 °C (hexane); $[\alpha]_D^{20}$ = + 7.5 (c 1.0, MeOH) or $[\alpha]_D^{20}$ = -8.5 (*c* 0.4, MTBE) {cf. lit. [8]: mp 111-113 °C; $[\alpha]_D^{25}$ = + 7.5 (*c* 1.0, MeOH)}; 99.6 % ee [chiral HPLC analysis; Daicel Chiralpack AD-RH (0.46 x 15 cm) column, column temperature 40 °C; eluent: water/isopropanol = 3:1; flow rate: 0.8 ml/min; UV detector 275 nm; t_R = 16.1 min (minor), t_R= 25.8 min (major)]. ^{1}H NMR ($CDCl_3$), δ: 2.00 (broad s, 2H, OH), 3.88 (dd, *J* = 11.6, 5.3 Hz; 1H, CH_2O), 3.97 (dd, *J* = 11.6, 3.2 Hz; 1H, CH_2O), 4.26-4.33 (m, 3H, CH_2O, CH), 6.87 (d, *J* = 7.5 Hz; 1H, $C^2_{Ar}H$), 7.39 (dd, *J* = 7.9, 8.2 Hz; 1H, $C^3_{Ar}H$), 7.47-7.53 (m, 3H, $C^{4,6,7}_{Ar}H$), 7.83 (d, *J* = 8.0 Hz; 1H, $C^5_{Ar}H$), 8.24 (d, *J* = 8.0 Hz; 1H, $C^8_{Ar}H$). ^{13}C NMR δ: 63.8 (CH_2OH), 69.3 (OCH_2), 70.6 (CH); 105.1, 120.8, 121.5, 125.3, 125.5, 125.6, 126.4, 127.5, 134.5, 154.0 (naphthyl).

***rac*-3-(4-Indolyloxy)-propane-1,2-diol, *rac*-4** was prepared by analogy with the published method [13]. To a stirred suspension of 1.3 g (9.4 mmol) K_2CO_3 in 5 ml CH_3CN a solution of 250 mg (1.9 mmol) 4-hydroxyindole in 3 ml CH_3CN was added dropwise within 10 min and the resulting mixture was stirred and heated under reflux for 2 h. Then 0.243 g (2.2 mmol) of racemic 3-chloropropane-1,2-diol was added dropwise and the mixture was further stirred and heated under reflux for 16 hours. The reaction mixture was filtrated and concentrated under reduced pressure to give a brown oil. The crude product was purified by column chromatography (silica gel, acetone-hexane, 1:3-1:1) and was crystallized in Et_2O. Yield 268 mg (69 %); mp 95-97 °C (Et_2O-MeCN) (lit. [13]: mp 96-98 °C). ^{1}H NMR (DMSO-d_6) *δ*: 3.49-3.52 (m, 2H), 3.82-3.88 (m, 1H), 3.96 (dd, *J* = 9.9, 5.9 Hz; 1H, CH_2O), 4.08 (dd, *J* = 9.6, 4.5 Hz; 1H, CH_2O), 4.63 (br.s, 1H, OH), 4.91 (br.s, 1H, OH), 6.43–6.48 (m, 2H), 6.95-6.98 (m, 2H), 7.19 (t, *J* = 2.7 Hz; 1H), 11.0 (br.s, 1H, NH). ^{13}C NMR δ: 63.4 (CH_2OH), 69.9 (OCH_2), 70.6 (CH); 99.0, 100.4, 105.2, 118.9, 122.2, 123.8, 137.8, 152.6 (indolyl).

(*R*)-3-(4-Indolyloxy)-propane-1,2-diol, (*R*)-4 was prepared from 4-hydroxyindole (250 mg, 1.9 mmol) and (*R*)-3-chloropropane-1,2-diol (0.243 g, 2.2 mmol), as described above for *rac*-**4**. The yield was 318 mg (82 %); mp 122-123 °C (Et_2O-MeCN, 3:1 v/v); $[\alpha]_D^{20}$ = –5.2 (*c* 1.5, MeOH); 95 % ee [chiral HPLC analysis; Daicel Chiralpack AD-RH (0.46 x 15 cm) column; column temperature 30 °C; eluent: isopropanol/water =1:3; flow rate: 0.4 ml/min; UV detector 275 nm; t_R = 10.1 min (major), t_R = 14.4 min (minor)] {lit. [9] for (*S*)-**4**: mp 119-120 °C; $[\alpha]_D^{20}$ = +5.1 (*c* 1.47, MeOH)}. ^{1}H and ^{13}C NMR spectra were identical with that cited above for *rac*-**4**.

(*S*)-3-(4-Indolyloxy)-propane-1,2-diol, (*S*)-4 was prepared from 250 mg (1.9 mmol) 4-hydroxyindole and (*S*)-3-chloropropane-1,2-diol (0.243 g, 2.2 mmol), as described above

for *rac*-**4**. The yield was 310 mg (80 %); mp 122 °C (Et_2O-MeCN, 3:1 v/v); $[\alpha]_D^{20}$ = +5.2 (*c* 1.49, MeOH); 96 % ee {lit. [9]: mp 119-120 °C; $[\alpha]_D^{20}$ = +5.1 (*c* 1.47, MeOH)}. ^1H and ^{13}C NMR spectra were identical with that cited above for *rac*-**4**.

Using the slightly nonracemic sample we have examined **entrainment effect for 3-(4-indolyloxy)-propane-1,2-diol**, **4**. Nonracemic sample of 3-(4-indolyloxy)-propane-1,2-diol (*S*)-**4** (0.2 g, 15% *ee*) was dissolved in a mixture of Et_2O (2.5 ml) and CH_3CN (1.5 ml) at 40 °C. The solution was cooled to r.t. and seeded with finely-pulverized (*S*)-**4** (1 mg, 96% *ee*). After standing the mixture for 17 h at -18 °C, precipitated (*S*)-**4** was collected by filtration (28 mg after drying; 89% *ee*). For monitoring the entrainment process during seed-induced crystallization "chiral" HPLC analysis of mother liquor has been used. It was found that after the removing of crystalline precipitate the mother liquor was enriched with (*R*)-**4** (5% *ee*). This solution was partly evaporated, then cooled and seeded with finely-pulverized (*R*)-**4** (1 mg, 95% *ee*). After standing overnight at -18 °C, 26 mg of (*R*)-3-(4-indolyloxy)-propane-1,2-diol (33% ee) was collected by filtration. Simultaneously the mother liquor was enriched with (*S*)-**4** (5% *ee*). Thus, the full cycle of resolution by entrainment has been demonstrated. Unfortunately, scarcity of initial material had prevented a bulk experiment.

2.3. X-ray analysis

The X-ray diffraction data for the crystals of 3-aryloxysubstituted glycerol ethers (*S*)-**3**, *rac*-**3** were collected on a «Enraf-Nonius CAD-4» automatic diffractometer using graphite monochromated CuK_α (1.54184 Å) radiation at 296 K. Data collection, editing and refinement parameters of the unit cell are carried out using program MolEN [14]. The X-ray diffraction data for the crystal of (*R*)-**4** was collected on a Bruker Smart Apex II CCD diffractometer using graphite monochromated MoK_α (0.71073 Å) radiation at 296 K. Data collection: images were indexed and integrated using the APEX2 data reduction package [15], the SADABS program [16] was used for absorption correction.

The crystal data, data collection, and the refinement parameters are given in Table 1. The structures were solved by direct method using program SIR [17] for (*S*)-**3**, *rac*-**3** and using SHELXS [18] program for (*R*)-**4**, and refined by the full matrix least-squares using SHELXL [19] programs. All non-hydrogen atoms were refined anisotropically.

The positions of the hydrogen atoms of amino and hydroxyl groups were determined based on the electronic density distribution and were refined isotropically. The others hydrogen atoms were inserted at calculated positions and refined as riding atoms. The absolute structure of the single crystal of 3-aryloxysubstituted glycerol ether (*S*)-**3** was determined on the basis of the Flack [20] parameter.

All calculations were performed on PC using WinGX [21] suit of programs. Analysis of the intermolecular interactions was performed using the program PLATON [22]. Mercury program package [23] was used for figures preparation.

The X-ray phase studies for the *rac*-**4** samples were performed on Bruker *D*8 Advance diffractometer equipped with Vario attachment and Vantec linear PSD, using $CuK_{\alpha 1}$ radiation (40 kV, 40 mA) monochromated by the curved Johansson monochromator (λ = 1.5406 Å). Room-temperature data were collected in the reflection mode with a flat-plate sample. The samples were loaded into a standard sample holder or on a glass plate, which was kept spinning (15 rpm) throughout the data collection. Patterns were recorded in the 2Θ range between 3 and 60°, in 0.008° steps, with a step time of 0.3-1.0 s. Five powder patterns were collected and summed for sample.

Crystallographic data (excluding structure factors) for the structures (*R*)-**4**, (*S*)-**3** and *rac*-**3** have been deposited in the Cambridge Crystallographic Data Centre as supplementary publication nos. CCDC 924943 - 924945 respectively. Copies of the data can be obtained free of charge upon application to the CCDC (12 Union Road, Cambridge CB2 1EZ UK. Fax: (internat.) +44-1223/336-033; E-mail: deposit @ccdc.cam.ac.uk).

Table 1. Crystallographic data for diols (*S*)-**3**, *rac*-**3**, and (*R*)-**4**.

Compound Formula	(*S*)-**3** $C_{13}H_{14}O_3$	*rac*-**3** $C_{13}H_{14}O_3$	(*R*)-**4** $C_{11}H_{13}NO_3$
M (g/mol)	218.24	218.24	207.22
Temperature, K	296(2)	296(2)	296(2)
Crystal class	Orthorhombic	Orthorhombic	Orthorhombic
Space group	$P2_12_12_1$	Pbca	$P2_12_12_1$
Crystal size	0.30 x 0.30 x 0.50 mm^3	0.04 x 0.40 x 0.45 mm^3	0.13 x 0.17 x 0.55 mm^3
Z, Z´	4, 1	8, 1	4, 1
Cell parameters	a = 5.011(1)Å b = 7.528(10)Å c = 29.549(3)Å	a = 7.929(5)Å b = 8.597(5)Å c = 33.42(2)Å	a = 4.9639(2)Å b = 7.3670(3)Å c = 28.093(1)Å
V, $Å^3$	1115(1)	2278(2)	1027.34(7)
F(000)	464	928	440
ρ_{calc} g/cm^3	1.300	1.273	1.340
μ, cm^{-1}	0.750	0.734	0.098
θ range, deg	$2.99 \leq \theta \leq 74.40$	$5.29 \leq \theta \leq 74.29$	$2.86 \leq \theta \leq 31.19$
Reflections measured	4995	2308	7561
Independent reflections	2256 [R(int) = 0.0278]	2307 [R(int) = 0.0169]	3276 [R(int) = 0.0439]
Number of parameters / restraints	154/0	154 / 0	148 / 0
Reflections [$I>2\sigma(I)$]	2174	1194	2490
Flack parameter	-0.2(1)	-	-
R_1 / wR_2 [$I>2\sigma(I)$]	0.0284 / 0.0770	0.0549 / 0.1347	0.0439/ 0.0964
R_1 / wR_2 (all reflections)	0.0296 / 0.0781	0.1301 / 0.1721	0.0624/ 0.1060
Goodness-of-fit on F^2	1.027	0.959	1.047
ρ_{max}/ρ_{min} ($eÅ^{-3}$)	0.126 / -0.110	0.206 / -0.204	0.152/ -0.144

3. Discussion

3.1. Synthesis

All the investigated samples were obtained by the uniform procedure by reacting a corresponding phenol with 3-chloropropane-1,2-diol **5** in the presence of a base. Scalemic chloropropanediols **5** of preassigned configuration were obtained by partial stereoselective hydrolysis of racemic epichlorohydrin according to the procedure developed by Jacobsen et al. [11]. The use of *rac*-**5** leads to the racemates, and the use of (*S*)- and (*R*)-3-chloropropane-1,2-diol **5** gives, respectively, target diols (*S*)-**3**, (*S*)-**4** and (*R*)-**4**:

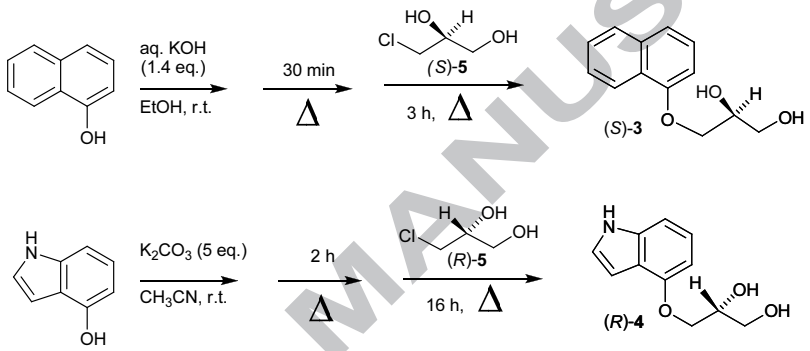

Scheme 2. Synthetic approaches to the compound studied.

3.2. IR spectra comparison

For the initial evaluation of the racemic variant of our studied compounds, we compared the IR spectra of the pairs of racemic and highly enantiomerically enriched crystalline samples of **3** and **4** in KBr pellets (Fig. 1).

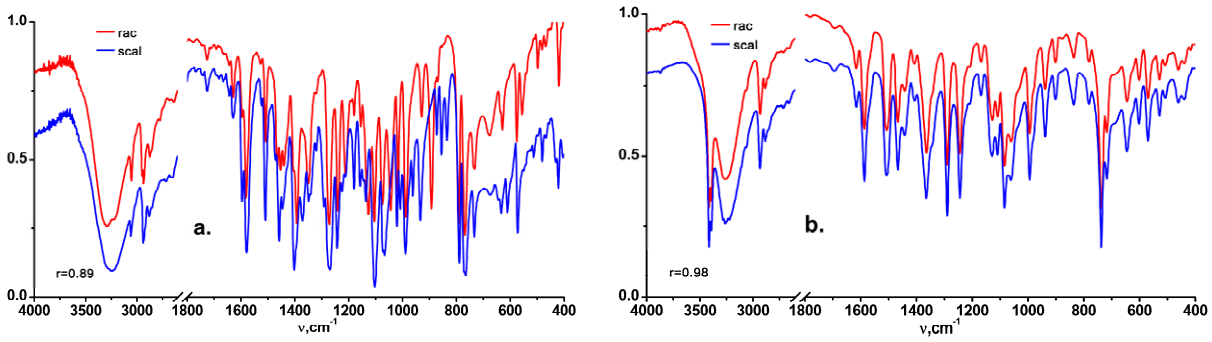

Figure 1. Comparison of the IR spectra of the crystalline samples (in KBr pellets) for chiral diols **3** (**a**) and **4** (**b**). Red curves belong to racemic samples; blue curves belong to scalemic samples.

The IR spectra of the optically active (scalemic) and racemic forms should be identical for the normal conglomerate (and in some extent for the solid solution) formative compounds. As a quantitative measure of similarity of the spectra, we have used the standard Pearson correlation coefficient **r** between two vectors $\{A_i^R\}$ and $\{A_i^S\}$, were A_i represents extinction corresponding to a given vibration frequency ν_i for real 2D arrays (A_i,ν_i) of digital spectra of the racemic (upper index R) and highly enantioenriched scalemic (upper index S) samples. The value $\mathbf{r}(A^R,A^S)=1$ corresponds to a perfect correlation of two vectors (identity of the spectra in our case). The comparison procedure is described in more details in our preceding works [24]; the **r** values obtained for the pairs of racemic and highly enantiomerically enriched samples of compounds **3** and **4** are 0.89 and 0.98 correspondingly. Based on these data, it is possible to assume that naphthyloxydiol **3** crystallizes to form a racemic compound. At the same time there is a substantial likelihood that indolyloxydiol **4** is a conglomerate forming compound.

3.3. Thermochemical data

The DSC measured melting points and enthalpies of fusion of *rac*-**3**, *rac*-**4**, (*S*)-**3** and (*R*)-**4** (96.9, 97.5, 110.8, and 121.5 °C; 32.2, 20.8, 39.0, and 34.7 $kJ \cdot mol^{-1}$ for the samples in the order listed) have been used for the construction of the binary phase diagrams for chiral diols **3** and **4** (Figure 1). The basic literature on the subject and formulas used for calculations has been described in detail in our resent review [25].

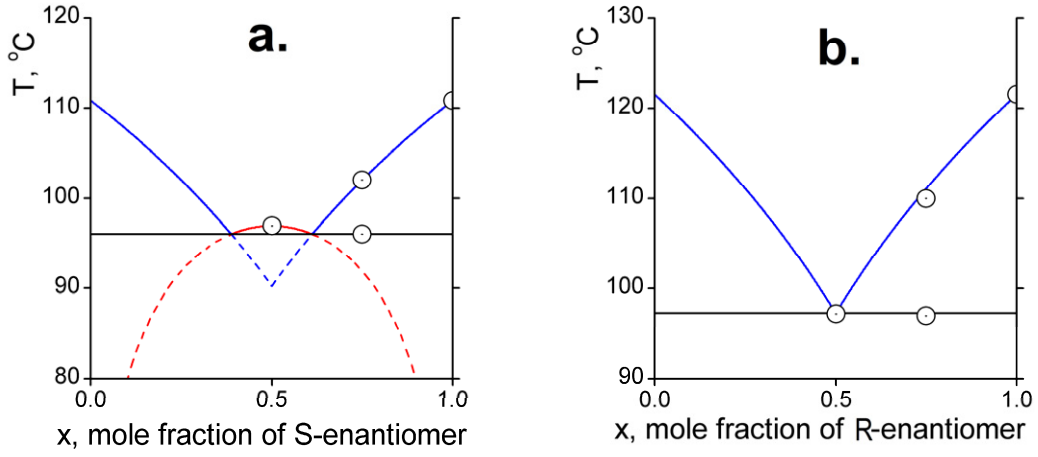

Figure 2. Binary melting phase diagrams for chiral diols **3** (a) and **4** (b). Circles: experimental points; blue lines: calculated Schröder-Van Laar curves branches; red line: calculated Prigogine-Defay curve.

The W-shaped phase diagram form with an ill-defined middle cupola is indicative of a weakly stable racemic compound formation from enantiomers of naphthyloxy derivative **3** in the solid state

(the calculated value of free energy for the process ΔG^0 = -720 J·mol^{-1}). The eutectic for **3** (T^f_{eu} = 96.0 °C) is composed of 0.62 mole fraction of a predominant enantiomer and of 0.38 mole fraction of another one as determined by the cross point for different liquidus legs position. Hence, the samples having initial *ee* value slightly higher than 0.24 could be extra enantioenriched during recrystallization.

In the transition from the naphthyloxy to indolyloxy substituted diol **4** the phase diagram transformed, acquiring V-shaped. The dome in the middle disappears, and the branches of the liquidus line converge at x = 0.5. The intersection of the theoretical curves is characterized by the value of 97.2 ° C on the temperature axis, which is almost identical to the experimental eutectic melting point T^f_{eu} = 97.5 °C. The calculated entropy of mixing of enantiomers in the liquid state is equal to ΔS^m_l = 5.23 J·K^{-1}·mol^{-1}, which is close to theoretical value of Rln2 for an ideal solution of conglomerate. Thus, in accordance with the above described IR data, 3-(4-indolyloxy)-propane-1,2-diol, a synthetic precursor of API pindolol, crystallizes to form a conglomerate. This fact allows believing that racemic **4** can be resolved into individual enantiomers by direct methods based on the stereoselective crystallization.

It is known that not every conglomerate formative racemic substance can be resolved by a preferential crystallization approach [25,26]. Therefore, we realized an attempt of a two-step experiment which has demonstrated the entrainment effect during the crystallization of slightly enantioenriched diol **4** solutions. The experiment (see experimental part) showed that the enriched in (+)-enantiomer solution after seeded crystallization become enriched in (-)-enantiomer, and then seeded crystallization of (-)-enantiomer again enriches the mother liquor in (+)-enantiomer. Unfortunately, there were only small quantities of *rac*-**4** at our disposal. For this reason it was impossible to carry out cyclic crystallization further. However, the very fact of the mother liquor change of the sign of rotation of the polarization plane gives us hope for the success of resolution by entrainment in preparative scale.

3.4. Single crystal X-ray investigations

The experimental details of the crystallographic experiments are listed in Table 1. No abnormal structure parameters (bond lengths and bond angles) were found for all three substances studied.

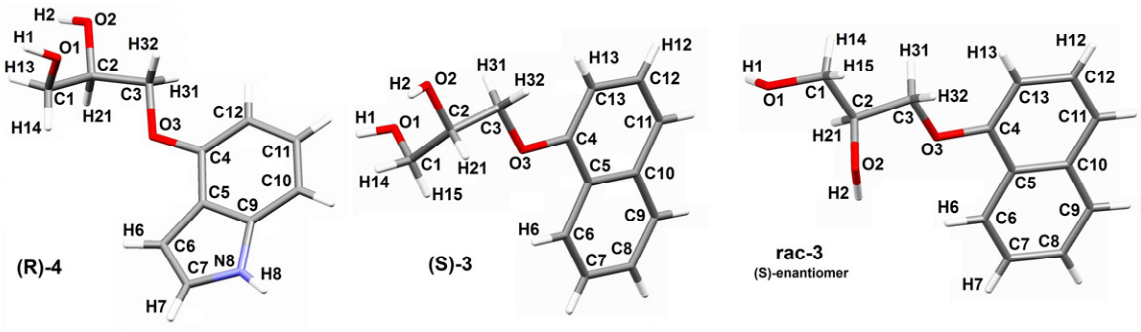

Figure 3. Molecular structure and numbering scheme for the symmetry independent molecules in scalemic [(*R*)-**4** and (*S*)-**3**] and racemic [*rac*-**3**, (*S*)-enantiomer is shown for ease of comparison] samples of the investigated aryloxypropanediols.

*3.4.1. (R)-3-(4-Indolyloxy)-propane-1,2-diol,(R)-**4***

A single crystal suitable for X-ray analysis we were able to prepare only for enantiopure indolyloxy substituted diol (*R*)-**4**. However, a comparison of the experimental powder diffraction pattern for the *rac*-**4** sample with the pattern, theoretically calculated from single crystal data for (*R*)-**4**, shows the identity of the crystal structures of the racemic and scalemic samples (Fig. 4). This special feature is inherent in conglomerate formative substances.

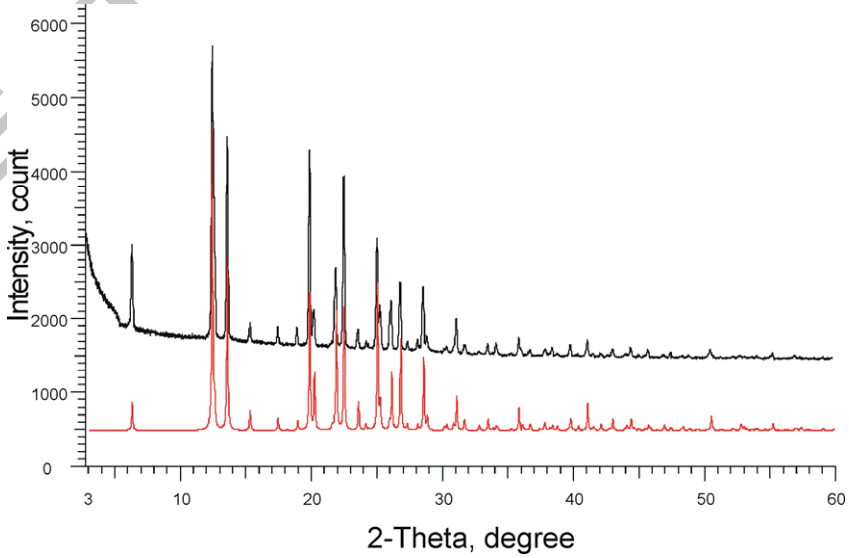

Figure 4. Calculated X-ray powder pattern of (*R*)-**4** (red) and experimental X-ray powder pattern of *rac*-**4** (black) at 296 K.

Analysis of crystallographic data for scalemic diol **4** identifies a set of classic intermolecular hydrogen bonds and C-H··· π interactions, which play an important role in the formation of the crystal packing (Table 2).

Table 2. Parameters of the intermolecular H-bonds and H··· π interactions for compound (*R*)-**4** in crystals.

D–H···A	D–H, Å	H···A, Å	D···A, Å	∠ DHA, °	Symmetry operation
O1-H1···O2	0.87(2)	1.84(2)	2.687(2)	166(2)	2-x,-1/2+y,3/2-z
O2-H2···O1	0.95(2)	1.76(2)	2.701(2)	179(2)	1+x,y,z
N8-H8···N8	0.89(3)	2.37(3)	3.256(2)	172(2)	-1/2+x,3/2-y,2-z
	H···Cg, Å	∠ N-H···Cg, °		N···Cg	Symmetry operation
N8-H8→ Cg	2.54(3)	147(2)		3.323(2)	-1/2+x,3/2-y,2-z

Cg = center of gravity of the fragment N8-C7-C6-C5-C9

System of intermolecular hydrogen bonds O-H···O generates primary supramolecular crystal-forming motif for (*R*)-**4**, namely infinite homochiral bilayer, which projections are shown in Figure 5. In short, the bilayer is formed by a 1D spiral system of H-bonds located along 2_1 screw axes; (*R*)-enantiomers form left-handed *M*-helix. Bilayer extends parallel to the plane *a0b*. Only glycerol fragments of the molecules are involved in the formation of the bilayer, whereas aromatic fragments are concentrated at the periphery.

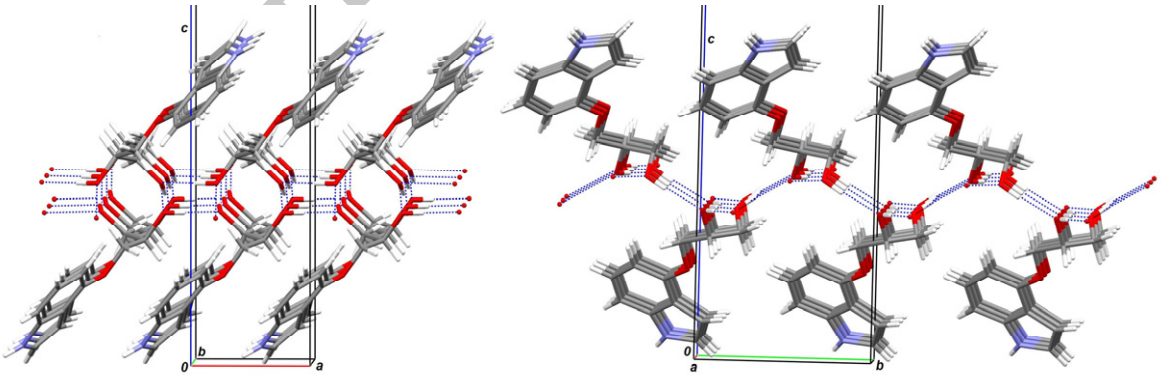

Figure 5. The main supramolecular motif in the (*R*)-**4** crystals: 2D bilayer formed by spiral intermolecular H-bond sequences located along 2_1 screw axes. Hydrogen bonds are depicted by blue dashed lines; view along *0b* and *0a* axes.

This supramolecular motif is common in the family of terminal aromatic glycerol ethers (TAGE) [25]. An example of this structure was observed for the first time for conglomerate formative chiral drug guaifenesin [27]. We named the motif as "guaifenesin-like" and described it

in detail in our preceding papers [28,29]. The crystal structure of (*R*)-**4** is interesting because it enlightens the way of combining the individual 2D bilayers in a three-dimensional network. The main role in this effect belongs to N-H bonds. They are capable of forming infinite chains of hydrogen bonds N-H···N (as illustrated in Fig. 6) as well as N-H ··· π contacts with the indole fragments belonging to adjacent layers (π-stacking of edge-to-face type or T-shaped π-interaction; see Tab. 2). Packing index in the (*R*)-**4** crystals is 68.7%.

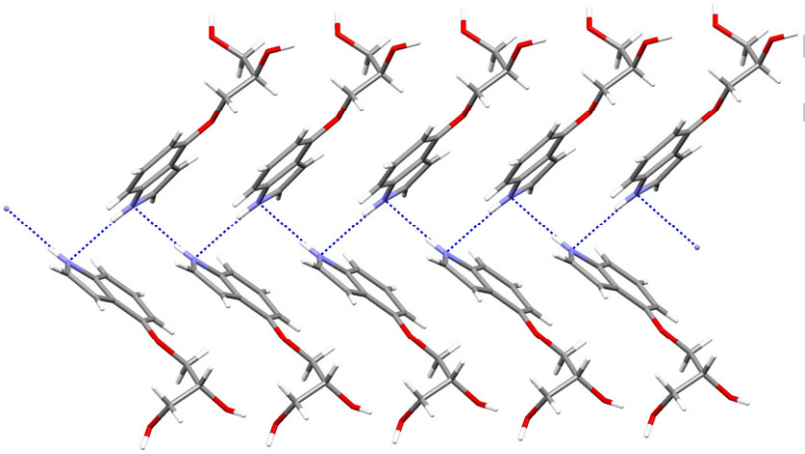

Figure 6. The N-H···N hydrogen bonds between neighboring bilayers in the (*R*)-**4** crystals; view along *0b* axis.

*3.4.2. (S)-3-(1-Naphthyloxy)-propane-1,2-diol, (S)-**3***

Enantiopure naphthyloxy diol **3** has many common structural features with indolyloxy diol **4**. Not surprisingly, that crystallizing in the same Sohncke space group $P2_12_12_1$, (*S*)-**3** molecules form the same main supramolecular motif, as (*R*)-**4** molecules do. Moreover, the unit cell parameters are very close between these two compounds (Tab. 1). The only significant difference between them consist with their chirality senses: (*S*)-enantiomers of diol **3** form a right-handed *P*-spiral 1D H-bonded columns within the 2D bilayers. Close to each other are the parameters of the intermolecular hydrogen bonds that provide the physical strength of the supramolecular bilayer (cf. Tab. 3 and Tab. 2).

Table 3. Parameters of the intermolecular H-bonds and C-H··· π interactions for (*S*)-**3** crystals.

D–H···A	D–H, Å	H···A, Å	D···A, Å	∠ DHA, °	Symmetry operation
O1-H1···O2	0.87(2)	1.86(2)	2.726(4)	170(1)	1-x,-1/2+y,1/2-z
O2-H2···O1	0.89(2)	1.83(2)	2.725(4)	176(2)	1+x,y,z
	H···Cg, Å	∠ C-H···Cg, °		C···Cg	Symmetry operation
C3-H32→ Cg	2.78	143		3.599(5)	1+x,y,z

Cg center of gravity of the fragment C4-C5-C10-C11-C12-C13

No other classical hydrogen bonds, except ones involved in the formation of supramolecular primary motif, present in the (*S*)-**3** crystals. During the formation of the crystal packing adjacent layers are connected to each other by the dispersion interactions of hydrophobic periphery and weak C-H···π contacts. That is, in contrast to the strong binding of bilayers for the indole derivative 4, in crystals of naphthyl derivative 3 the bilayers are weakly related. Packing indices for the compounds (*S*)-**3** (68.5%) and (*R*)-**4** (68.7%) are almost identical. Despite this, the indole derivative **4** undergoes spontaneous resolution (that is, generates homochiral packing during racemate crystallization), whereas naphthalene derivative **3** has not. It is possible that the lack of directional interactions, which connect the primary fragments, determines the type of crystallization for racemates of the compounds **3** and **4**.

*3.4.3. rac-3-(1-Naphthyloxy)-propane-1,2-diol, rac-**3***

The differences between the crystal structure of the racemic and scalemic naphthyloxy substituted diols **3** could be detected already at the level of conformation of the crystal forming molecules (Fig. 3). In the crystals of most (but not all) of the studied terminal aromatic glycerol ethers, and in particular, in the crystals of (*R*)-**4** and (*S*)-**3**, four atoms form all-trans chain C4O3C3C2O2 within the acyclic fragment. In the crystals of *rac*-**3** five atoms form the all-trans chain C4O3C3C2C1O1. As a result, all of non-hydrogen atoms, except for O2, lie almost in the same plane, which includes (along with hydrogen atoms H6-H13 of the naphthyl fragment) 22 atoms. Atoms C1 (0.096Å), C2 (0.092Å) and C3 (0.095Å) deviate to the greatest extent from the calculated plane.
Analysis of crystallographic data for *rac*-**3** identifies a set of classic intermolecular hydrogen bonds of O-H···O type (Table 4), which differs from discussed above.

Table 4. Parameters of the intermolecular H-bonds for compound *rac*-**3** in the crystal.

D–H···A	D–H, Å	H···A, Å	D···A, Å	∠ DHA, °	Symmetry operation
O1-H1···O2	1.03(4)	1.72(4)	2.729(3)	167(3)	1/2+x,y,1/2-z
O2-H2···O1	0.98(3)	1.76(3)	2.718(3)	167(3)	1-x,-1/2+y,1/2-z

These H-bonds generate new packing, not previously encountered in the series of TAGEs. The main supramolecular crystal forming motif for racemic naphthyloxy diol is a parallel to *a0b* plane bilayer, occupying a limited (~ 16.5Å) space along *0c* axis (Fig. 7a,b) and extending infinitely in the *0a* and *0b* directions (Fig. 7c).

Bilayer fastening system of hydrogen bonds represents the infinite zigzag chains, oriented along the 2_1 screw axes, parallel to the *0b* direction. By virtue of symmetry (space group Pbca), it creates conditions for a single bilayer division into zones (stripes, ribbons), formed by the

enantiomers of common configuration. This is clearly seen in the projections along the *0b* (Fig. 8a) and *0c* directions. Within the crystal lattice the primary bilayers are fastened together by the dispersion and hydrophobic interactions of aromatic fragments, gathered in the periphery of the bilayer. The presence of an inversion center in the center of the unit cell forces the neighboring bilayers touch each other with the fragments containing molecules with the opposite configurations. Thus, it turns out that the elongated in the *0b* direction endless homochiral stripes are shifted by half a period in the *0a* and *0c* directions (Fig. 8b).

Figure 7. The main supramolecular motif in the *rac*-**3** crystals: 2D bilayer formed by zigzag chains of intermolecular H-bond sequences located along 2_1 screw axes parallel to *0b* direction. Hydrogen bonds are depicted by blue dashed lines; view along *0a* (**a**), *0b* (**b**), and *0c* (**c**) axes.

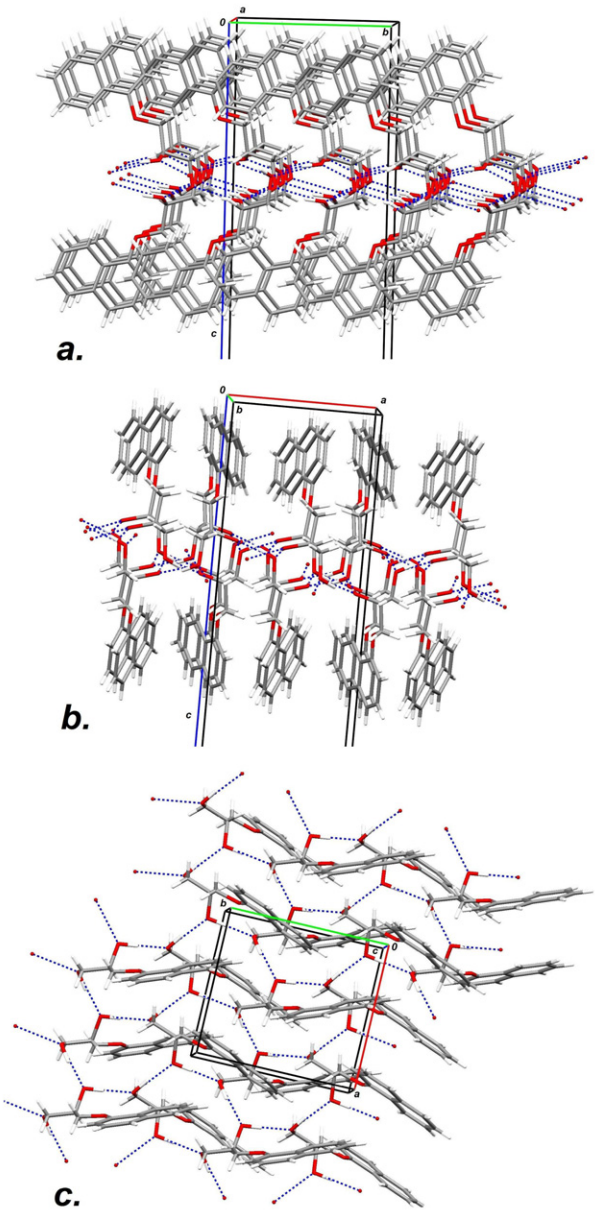

The low packing index (equal to 67%) points on the loose nature of the *rac*-**3** crystal packing. Thus, compound **3** is an example of a violation of Wallach rule [30,31], according to which the density of racemic crystal is greater than the density of homochiral crystal for the same substance. However, a racemate of compound **3** crystallized from solution or melt to form a racemic compound, not a racemic conglomerate. We found no obvious crystallographic conditioning factors for this phenomenon. Apparently to explain the behavior of *rac*-**3** the need exists to turn to other arguments. First of all, the formation of racemic crystals from a racemic feed material is always encouraged by the kinetic effects, well described in Brock et al. paper [31]. These effects may be negligible in the significant differences in the energy of the homo- and heterochiral crystal packing. But they can determine the result of crystallization in borderline cases, to which the crystallization of compound **3** clearly belongs.

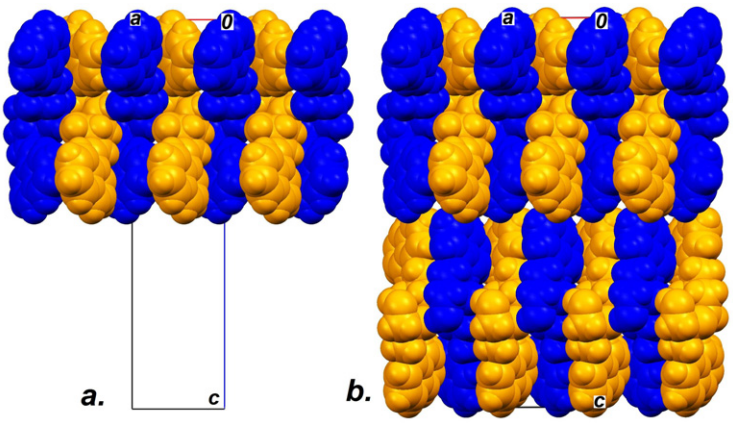

Figure 8. Segmentation of the 2D bilayer on to homochiral zones (**a**), and the mode of the bilayers combination within the unit cell (**b**) of *rac*-**3** crystal. View along *0b* axis; (*R*)-enantiomers are depicted in orange color, (*S*)-enantiomers are depicted in blue.

4. Conclusions

Synthetic precursors of valuable chiral drug substances propranolol **1** and pindolol **2**, 3-(1-naphthyloxy)-propane-1,2-diol **3** and 3-(4-indolyloxy)-propane-1,2-diol **4**, crystallizing from enantiopure starting materials, form a very similar "guaifenesin-like" crystal packing. In both cases the basic supramolecular motif appears to be 2D bilayer, formed by a sequence of 1D spiral intermolecular hydrogen bonds located along 2_1 screw axes; in both cases (*R*)-enantiomers form left-handed *M*-helixes and (*S*)-enantiomers form right-handed *P*-helixes. Only glycerol fragments of the molecules are involved in the formation of the bilayer, whereas aromatic fragments are concentrated at the periphery. In the case of indole derivative **4** primary 2D bilayers are combined into 3D crystal structure mainly due to N-H···N hydrogen bonds between indole fragments of adjacent bilayers. There are no classic hydrogen bonds and/or other directional interactions, which connect the primary fragments in the 3D crystal structure of naphthalene derivative **3**. These differences are responsible for the different crystallization behavior of racemic samples of **4** and **3**. Under these conditions indolyloxy diol **4** forms the enantiopure crystalline phase, that is, acts as a conglomerate formative compound. Naphthyloxy diol **3**, being crystallized from the racemic feed material, forms weakly stable racemic compound with rather loose crystal packing. The predominant formation of the racemic compound, not racemic conglomerate, in the case of *rac*-**3** may be due to kinetic effects, which always promotes a racemic compound formation during crystallization from a racemic substrate.

Acknowledgment

The authors thank the Russian Fund of Basic Research for financial support (Grant number 13-03-00174). The authors thank Drs. Alexander Pashagin and Rimma Eliseenkova for valuble technical assistance.

References

[1] The Merck Index. 14th ed., Ed. M. J. O'Neil, Merck and Co., Inc.: Whitehouse Station, NJ, USA, 2006, (a) 7840; (b) 7443.

[2] R. Mehvar, D.R. Brocks, J. Pharm. Pharm. Sci. 4 (2001) 185.

[3] K. Stoschitzky, W. Lindner, Wien. Med. Wochenschr. 140 (1990) 156.

[4] (a) T. Rodgers, D. Leahy, M. Rowland, J. Pharm. Sci. 94 (2005) 1237;
(b) J.M. Monti, H. Jantos, Neuropharmacology 33 (1994) 705.

[5] S.H. Neau, M.K. Shinwari, E.W. Hellmuth, Int. J. Pharm. 99 (1993) 303.

[6] A.A. Bredikhin, D.V. Savel'ev, Z.A. Bredikhina, A.T. Gubaidullin, I.A. Litvinov, Russ. Chem. Bull. 52 (2003) 853.

[7] Z.M. Wang, X.L. Zhang, K.B. Sharpless, Tetrahedron Lett. 34 (1993) 2267.

[8] Z.A. Bredikhina, D.V. Savel'ev, A.A. Bredikhin, Russ. J. Org. Chem. 38 (2002) 213.

[9] S. Iriuchijima, N. Kojima, Agric. Biol. Chem. 46 (1982) 1153.

[10] B.A. Czeskis, J. Labelled Compd. Radiopharm. 41 (1998) 465.

[11] S.E. Schaus, B.D. Brandes, J.F. Larrow, M. Tokunaga, K.B. Hansen, A.E. Gould, M.E. Furrow, E.N. Jacobsen, J. Am. Chem. Soc. 124 (2002) 1307.

[12] A.A. Bredikhin, Z.A. Bredikhina, V.G. Novikova, A.V. Pashagin, D.V. Zakharychev, A.T. Gubaidullin, Chirality 20 (2008) 1092.

[13] H. Sasai, Y.M.A. Yamada, T. Suzuki, M. Shibasaki, Tetrahedron 50 (1994) 12313.

[14] L.H. Straver, A.J. Schierbeek, MolEN, Structure Determination System, Program Description. Nonius B.V. Delft, vol. 1 (180). Netherlands, 1994.

[15] APEX2 (Version 2.1), SAINTPlus . Data Reduction and Correction Program (Version 7.31A), Bruker Advanced X-ray Solutions, Bruker AXS Inc., Madison, Wisconsin, USA, 2006.

[16] G.M. Sheldrick, SADABS, Program for empirical X-ray absorption correction. Bruker-Nonius, 1990-2004.

[17] A. Altomare, M.C. Burla, M. Camalli, G.L. Cascarano, C. Giacovazzo, A. Guagliardi, A.G.G. Moliterni, G. Polidori, R. Spagna, J. Appl. Cryst., 32 (1999) 115.

[18] G.M. Sheldrick, SHELXS 97 Program for Solution of Crystal Structure, University of Goettingen, Germany, **1997.**

[19] G.M. Sheldrick, SHELXL97 a Computer Program for Crystal Structure Determination, University of Gottingen, 1997.

[20] (a) H.D. Flack, Acta Crystallogr. A39 (1983) 876;
(b) H.D. Flack, G. Bernardinelli, J. Appl. Crystallogr. 33 (2000) 1143.

[21] L.J. Farrugia, J. Appl. Cryst. 32 (1999) 837.

[22] A.L. Spek, J. Appl. Cryst. 36 (2003) 7.

[23] (a) I.J. Bruno, J.C. Cole, P.R. Edgington, M.K. Kessler, C.F. Macrae, P. McCabe, J. Pearson, R. Taylor, Acta Cryst. B58 (2002) 389;
(b) C.F. Macrae, P.R. Edgington, P. McCabe, E. Pidcock, G.P. Shields, R.Taylor, M. Towler, J. van de Streek, J. Appl. Crystallogr. 39 (2006) 453.

[24] (a) A.A. Bredikhin, Z.A. Bredikhina, F.S. Akhatova, D.V. Zakharychev, E.V. Polyakova, Tetrahedron: Asymmetry 20 (2009) 2130;
(b) Z.A. Bredikhina, D.V. Zakharychev, A.T. Gubaidullin, A.A. Bredikhin, J. Mol. Struct. 936 (2009) 171.

[25] A.A. Bredikhin, Z.A. Bredikhina, D.V. Zakharychev, Mendeleev Commun. 22 (2012) 171.

[26] (a) G. Levilain, G. Coquerel, CrystEngComm. 12 (2010) 1983;
(b) S. Gonella, J. Mahieux, M. Sanselme, G. Coquerel, Org. Process Res. Dev. 16 (2011) 286.

[27] A.A. Bredikhin, A.T. Gubaidullin, Z.A. Bredikhina, D.B. Krivolapov, A.V. Pashagin, I.A. Litvinov, J. Mol. Struct. 920 (2009) 377.

[28] A.A. Bredikhin, A.T. Gubaidullin, Z.A. Bredikhina, J. Mol. Struct. 975 (2010) 323.

[29] A.A. Bredikhin, D. V. Zakharychev, Z.A. Bredikhina, A.T. Gubaidullin, R.R. Fayzullin, CrystEngComm. 14 (2012) 211.

[30] (a) O. Wallach, Lieb. Ann. Chem. 286 (1895) 90;
(b) O. Wallach, Lieb. Ann. Chem. 286 (1895) 119.

[31] C.P. Brock, W.B. Schweizer, J.D. Dunitz, J. Am. Chem. Soc. 113 (1991) 9811.

Table 1. Crystallographic data for diols (*S*)-**3**, *rac*-**3**, and (*R*)-**4**.

Compound Formula	(*S*)-**3** $C_{13}H_{14}O_3$	*rac*-**3** $C_{13}H_{14}O_3$	(*R*)-**4** $C_{11}H_{13}NO_3$
M (g/mol)	218.24	218.24	207.22
Temperature, K	296(2)	296(2)	296(2)
Crystal class	Orthorhombic	Orthorhombic	Orthorhombic
Space group	$P2_12_12_1$	Pbca	$P2_12_12_1$
Crystal size	0.30 x 0.30 x 0.50 mm^3	0.04 x 0.40 x 0.45 mm^3	0.13 x 0.17 x 0.55 mm^3
Z, Z´	4, 1	8, 1	4, 1
Cell parameters	a = 5.011(1)Å b = 7.528(10)Å c = 29.549(3)Å	a = 7.929(5)Å b = 8.597(5)Å c = 33.42(2)Å	a = 4.9639(2)Å b = 7.3670(3)Å c = 28.093(1)Å
V, $Å^3$	1115(1)	2278(2)	1027.34(7)
F(000)	464	928	440
ρ_{calc} g/cm^3	1.300	1.273	1.340
μ, cm^{-1}	0.750	0.734	0.098
θ range, deg	2.99 ≤ θ ≤ 74.40	5.29 ≤ θ ≤ 74.29	2.86≤ θ ≤ 31.19
Reflections measured	4995	2308	7561
Independent reflections	2256 [R(int) = 0.0278]	2307 [R(int) = 0.0169]	3276 [R(int) = 0.0439]
Number of parameters / restraints	154/0	154 / 0	148 / 0
Reflections [I>2σ(*I*)]	2174	1194	2490
Flack parameter	-0.2(1)	-	-
R_1 / wR_2 [I>2σ(*I*)]	0.0284 / 0.0770	0.0549 / 0.1347	0.0439/ 0.0964
R_1 / wR_2 (all reflections)	0.0296 / 0.0781	0.1301 / 0.1721	0.0624/ 0.1060
Goodness-of-fit on F^2	1.027	0.959	1.047
ρ_{max}/ρ_{min} ($eÅ^{-3}$)	0.126 / -0.110	0.206 / -0.204	0.152/ -0.144

Table 2. Parameters of the intermolecular H-bonds and H··· π interactions for compound (*R*)-**4** in crystals.

D–H···A	D–H, Å	H···A, Å	D···A, Å	∠ DHA, °	Symmetry operation
O1-H1···O2	0.87(2)	1.84(2)	2.687(2)	166(2)	2-x,-1/2+y,3/2-z
O2-H2···O1	0.95(2)	1.76(2)	2.701(2)	179(2)	1+x,y,z
N8-H8···N8	0.89(3)	2.37(3)	3.256(2)	172(2)	-1/2+x,3/2-y,2-z
	H···Cg, Å	∠ N-H···Cg, °		N···Cg	Symmetry operation
N8-H8→ Cg	2.54(3)	147(2)		3.323(2)	-1/2+x,3/2-y,2-z

Cg = center of gravity of the fragment N8-C7-C6-C5-C9

Table 3. Parameters of the intermolecular H-bonds and C-H··· π interactions for (*S*)-**3** crystals.

D–H···A	D–H, Å	H···A, Å	D···A, Å	∠ DHA, °	Symmetry operation
O1-H1···O2	0.87(2)	1.86(2)	2.726(4)	170(1)	1-x,-1/2+y,1/2-z
O2-H2···O1	0.89(2)	1.83(2)	2.725(4)	176(2)	1+x,y,z
	H···Cg, Å	∠ C-H···Cg, °		C···Cg	Symmetry operation
C3-H32→ Cg	2.78	143		3.599(5)	1+x,y,z

Cg center of gravity of the fragment C4-C5-C10-C11-C12-C13

Table 4. Parameters of the intermolecular H-bonds for compound *rac*-**3** in the crystal.

D–H···A	D–H, Å	H···A, Å	D···A, Å	∠ DHA, °	Symmetry operation
O1-H1···O2	1.03(4)	1.72(4)	2.729(3)	167(3)	1/2+x,y,1/2-z
O2-H2···O1	0.98(3)	1.76(3)	2.718(3)	167(3)	1-x,-1/2+y,1/2-z

Highlights:

- Crystallization features of chiral drugs propranolol and pindolol precursors are investigated.
- 3-(4-Indolyloxy)-propane-1,2-diol is a conglomerate formative compound.
- Hydrogen N-H···N bonds are responsible for conglomerate stabilization.
- 3-(1-Naphthyloxy)-propane-1,2-diol forms weakly stable solid racemic compound.
- The predominant formation of the racemic compound may be due to kinetic effects.